JOINT INSTITUTE FOR NUCLEAR RESEARCH
Veksler and Baldin laboratory of High Energy Physics

FINAL REPORT ON THE INTEREST PROGRAMME

Phase dynamics of a stack of intrinsic SIS Josephson junctions

Supervisor:
Dr. Majed Nashaat AbdelGhani

Student:
Hala Alsayad, Egypt
Cairo University

Participation period:
February 13 - April 02, Wave 8

Dubna, 2023

Contents

Abstract

In this study we investigate the phase dynamics of a single superconductor-insulator-superconductor (SIS) junction and a stack of SIS junctions. Some interesting features appear for a stack of SIS junctions where a parametric resonance region is developed and the charge on the superconducting layers grows exponentially leading to the formation of a longitudinal plasma wave (LPW) along the c-axis of our stack. We also study the effect of external radiation on the current voltage characteristics (CVC) for both single and stack systems which shows a development of constant voltage steps (Shapiro steps).

Chapter 1

Single SIS Josephson junction

Prior to 1962 it was thought that for two weakly coupled superconductors, where the coupling can be through a thin insulating barrier (SIS junction), a normal metal barrier (SNS), or a ferromagnetic material (SFS), etc.., the probability of a Cooper pair tunneling across the barrier is insignificantly small. Thus at T=0 and for applied voltages less than twice the energy gap where no quasiparticles are present no current should be observed. In 1962 it was predicted by Brian D. Josephson that this indeed was not true and the Cooper pairs can tunnel through the barrier with a probability equal to that of a single quasiparticle and this effect was named after him.
Our study here concerns the Josephson effect for SIS junctions.

1.1 The Josephson equations

The main theoretical tools describing the Josephson effect are the two Josephson equations:
The current-phase relation

$$J_s(\phi) = J_c \sin\phi \tag{1.1}$$

where ϕ is the phase difference $\phi = \theta_2 - \theta_1$, θ_1 and θ_2 are the phases characterizing the macroscopic wave functions of the two superconductors $\psi_1 = \sqrt{n_s^{*1}}e^{i\theta_1}$, $\psi_2 = \sqrt{n_s^{*2}}e^{i\theta_2}$, n_s^{*1}, n_s^{*2} being the Cooper pair densities of the two superconductors.
J_s is the supercurrent density and J_c is a critical current density beyond which the current flowing cannot all flow as a supercurrent only, the excess

current has to flow through a resistive channel. This relation and the exact shape of the critical current density J_c can be derived from solving the Schrödinger equation for this tunneling problem, using wave matching in the three regions of superconductor 1, insulator, superconductor 2 and assuming a homogeneous barrier and homogeneous supercurrent flow. It was found that for a typical barrier of thickness of a few nm the critical current density decreases exponentially with increasing the barrier's thickness.
Here we deal with short Josephson junctions where the junction area is small enough so that the supercurrent density can be assumed constant and the current-phase relation takes the form

$$I_s(\phi) = I_c \sin \phi \tag{1.2}$$

The second Josephson equation is the voltage-phase relation relating the phase difference across the junction and the potential difference developed.

$$\frac{\partial \phi}{\partial t} = \frac{2\pi}{\Phi_o} V \tag{1.3}$$

where Φ_o is the flux quantum given by $\Phi_o = h/2e$.

1.2 AC and DC Josephson effects

Two very important effects occurring are:
The DC Josephson effect, where without the application of any external current or voltage, a DC supercurrent flows due to the tunneling of Cooper pairs, where ϕ is a constant since the supercurrent flowing is less than the critical current and no external biasing is present so no voltage is developed across the junction and thus the phase difference is a constant that doesn't depend on time.
The other is the AC Josephson effect, where for example on applying a DC voltage, an oscillating supercurrent is produced. Integrating Eq.(1.3) since V is constant yields

$$\phi(t) = \phi_o + \frac{2\pi}{\Phi_o} V\, t \tag{1.4}$$

Thus the Josephson supercurrent is time dependent $I_s(t) = I_c \sin \phi(t)$ oscillating with the Josephson frequency

$$\omega_J = \frac{2\pi}{\Phi_o} V \tag{1.5}$$

1.3 The superconducting state and the voltage state

So far we have been discussing cases where I_s does not exceed I_c, this state is referred to as the superconducting state or the zero voltage state where all the current flows as supercurrent and no voltage drop is developed across the junction. If the current exceeds such critical current, the excess flows through a resistive channel, the so called normal current channel creating a potential difference V and a time evolving phase difference. If the potential difference evolves in time as well, the excess current can also flow as a displacement current through a capacitive channel. This state is the so called voltage state. If the junction is biased using a DC current source whose value exceeds I_c, the rest flows through the resistive and capacitive channels and the total current is of course fixed by the fixed biasing current.

1.4 The model

According to our previous discussion an equivalent circuit [1] of the Josephson junction in the voltage state including all current contributions is of the form,

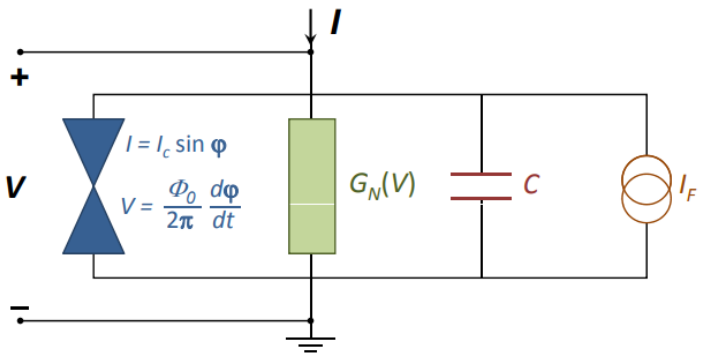

Figure 1.1: The equivalent circuit for a Josephson junction in the voltage state [1].

$$I = I_s + I_N + I_D + I_F \tag{1.6}$$

where I_F is a fluctuating noise current that we shall ignore in our treatment of a single junction. I_D is the displacement current given by $I_D = C\frac{dV}{dt}$, I_N

is the quasiparticle current given by $G_N(V)V$, where $G_N(V)$ is the normal conductance which we will take as a constant taking the resistively and capacitively shunted junction (RCSJ) Model approximation, $G_N(V) = G_N = \frac{1}{R_N}$, and I_s is the Josephson supercurrent $I_s = I_c \sin\phi$.
This combined with the Josephson voltage-phase relation Eq.(1.3) gives

$$\left(\frac{\hbar}{2e}\right) C\frac{d^2\phi}{dt^2} + \left(\frac{\hbar}{2e}\right)\frac{1}{R}\frac{d\phi}{dt} + I_c[\sin\phi - \frac{I}{I_c}] = 0 \tag{1.7}$$

This is a second order nonlinear differential equation which we solve numerically. We first need to rewrite it in a dimensionless form, this can be done by using the normalized time $\tau = t\omega_p$, where $\omega_p = \sqrt{2eI_c/\hbar C}$ is the so called plasma frequency which is the system's oscillation frequency with neglecting the first derivative of ϕ with respect to time, zero biasing current and for small ϕ such that $\sin\phi \simeq \phi$.
Substituting we get the dimensionless equation

$$\frac{d^2\phi}{d\tau^2} + \beta\frac{d\phi}{d\tau} + \sin\phi - i = 0, \tag{1.8}$$

where i is the biasing current I normalized to I_c and β is the so called dissipation parameter which is related to the Stewart-McCumber parameter $\beta_c = (2e/\hbar)\, I_c R_N^2 C$ by $\beta = 1/\sqrt{\beta_c}$.
We call junctions with ($\beta_c \ll 1$), ($\beta \gg 1$) or equivalently small capacitance and/or resistance, overdamped junctions. While for junctions with ($\beta_c \gg 1$) *or* ($\beta \ll 1$), or equivalently large capacitance and/or resistance, underdamped junctions.
The naming (overdamped/ underdamped) stems from a mechanical analogy to a system of a particle of mass M in a potential U with damping η whose equation of motion is given by

$$M\frac{d^2x}{dt^2} + \eta\frac{dx}{dt} + \vec{\nabla}U = 0. \tag{1.9}$$

Multiplying Eq.(1.7) by $\frac{\hbar}{2e}$ we get the equivalences

$$M = \left(\frac{\hbar}{2e}\right)^2 C, \qquad \eta = \left(\frac{\hbar}{2e}\right)^2 \frac{1}{R} \tag{1.10}$$

thus for small R and/or C it's overdamped, while for large R and/or C it's underdamped.

Equation (1.8) is the dimensionless nonlinear differential equation describing our system along with the Josephson voltage-phase relation Eq.(1.3). To obtain a CVC we solve Eq.(1.8) using a fourth order Runge-Kutta method. In our calculations, for each step of current Δi the voltage time dependence is calculated with a step of time $\Delta\tau$, then the average voltage over a time domain we choose is calculated and our CVC curve is developed between the time averaged voltage at each current point determined by Δi.

1.5 Overdamped and underdamped junctions

Here we study the CVC corresponding to a DC current source biasing of the Josephson junction. The current step was taken to be $\Delta i = 0.0005$, the step of time $\Delta\tau = 0.05$ and the time domain for averaging the voltage starts from 80 to 1000 for the overdamped case, and from 80 to 250 for the underdamped case.
For **strong damping** ($\beta_c \ll 1$), ($\beta \gg 1$) the CVC curve shown below consists of two regions.

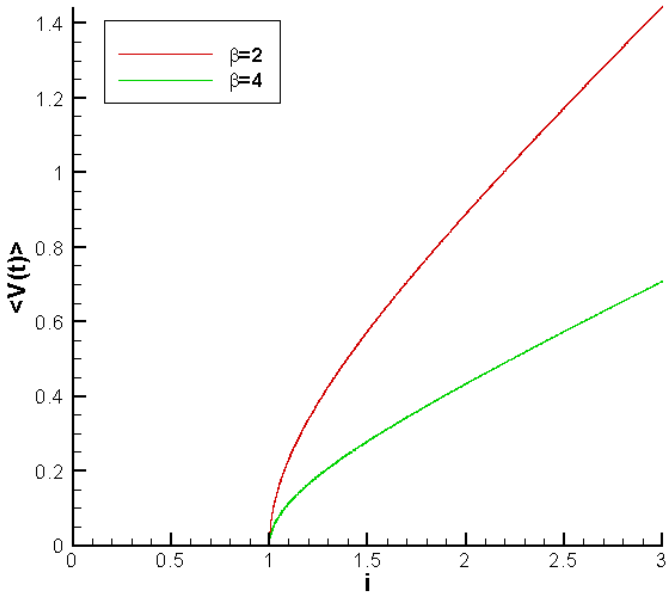

Figure 1.2: CVC for an overdamped junction with dissipation parameters $\beta = 2$ and $\beta = 4$.

The first one for $I < I_c$ i.e. $i < 1$, the Josephson junction is in the zero voltage state since all the current should be flowing as a Josephson supercurrent. For $I > I_c$ i.e. $i > 1$ and for $\beta \gg 1$ Eq.(1.7) is solved to give the time averaged voltage

$$< V(t) >= I_c R \sqrt{\left(\frac{I}{I_c}\right)^2 - 1}, \tag{1.11}$$

giving the behaviour shown above. As β is increased it can be seen that the curve shifts downward, this is directly shown through the R dependence in Eq.(1.11).

For **weak damping**, unlike the strong damping, the behavior will depend on the direction of current, as shown in the figure below this forms a hysteresis region. This hysteresis region can be understood from the mechanical

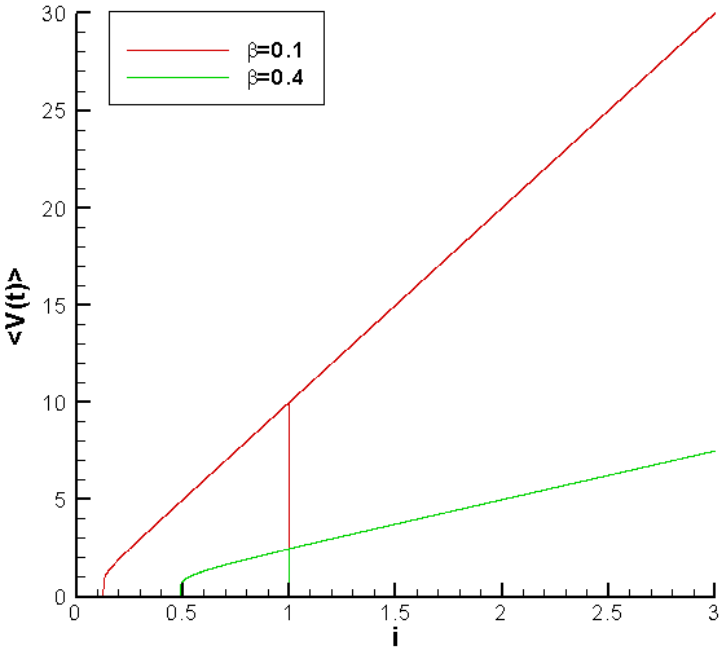

Figure 1.3: CVC for an underdamped junction with dissipation parameters $\beta = 0.1$ and $\beta = 0.4$.

analogue point of view that in the case of weak damping the particle would have a relatively large KE and so it returns to the zero voltage state at a

lower value of current than I_c, this value is called the return current and it tends to zero when $\beta \to 0$. The hysteresis region is larger ,of course, for lower dissipation parameter. It can also be seen that the behavior here is an ohmic one, this is because for an underdamped junction solving Eq.(1.8) for ($\beta_c \gg 1$) *or* ($\beta \ll 1$) yields an almost constant voltage resulting in a sinusoidal behavior for the Josephson supercurrent with about zero mean and thus almost all the current is carried by the resistive channel.

1.6 The effect of external radiation

The effect of external radiation is accounted for by adding the extra term $A \sin \omega\tau$ to the biasing current i, where ω is the frequency of the external radiation and A is its amplitude normalized to the critical current I_c. The figure shown is for the overdamped case with $\beta = 4$, $A = 1$, $\omega = 0.5$ and numerical parameters $\Delta i = 0.0005$, $\Delta\tau = 0.05$ and a time domain from about 1005 to about 12566. We observe constant voltage steps in the CVC curve.

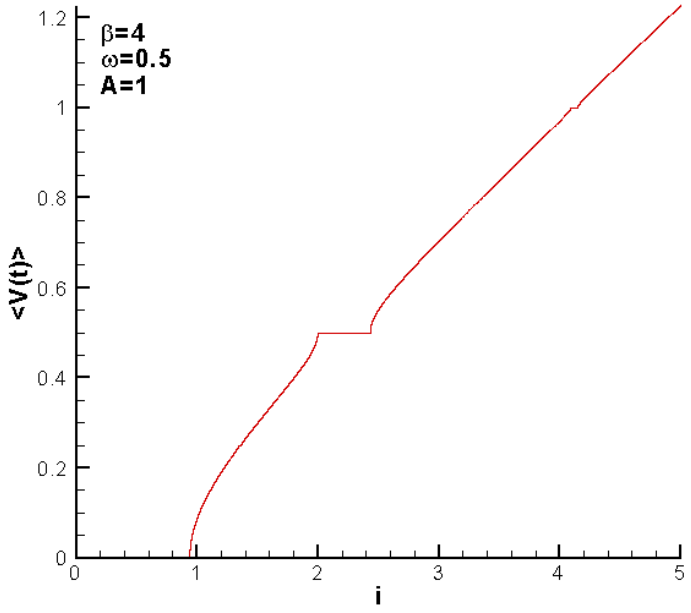

Figure 1.4: CVC for an overdamped junction with dissipation parameter $\beta = 4$, external radiation of amplitude $A = 1$ and frequency $\omega = 0.5$

These steps are the so called Shapiro steps. The condition for the appearance of such steps is when the normalized time averaged voltage is equal to the applied frequency ,normalized to the plasma frequency, or integral multiples of it i.e.

$$V_n = n\,\omega, \quad n = 1, 2, 3, .. \tag{1.12}$$

Here indeed we observe a step at $V_1 = 0.5$ and another at $V_2 = 2\omega = 1$.

Chapter 2

Stack of Josephson junctions (HTSCs)

We now deal with a stack of N SIS Josephson junctions,i.e. N+1 superconducting layers, instead of just a single junction. Some interesting features are developed. It can be seen from CVC curves that not all the junctions transition into the resistive state together, the transition is discrete. The CVC is characterized by a fundamental parametric resonance (fPR) where an exponential charge growth over each layer is developed and a longitudinal plasma wave is produced along the c-axis of the material whose frequency is half of that of the Josephson frequency at the fPR [2]. Another interesting feature also occurs on irradiating the stack with a frequency equal to that of the Josephson frequency, the so called double resonance condition, this leads to the appearance of constant voltage steps (Shapiro steps) at the fPR.

2.1 Intrinsic Josephson junctions

The layering structure of high temperature superconductors (HTSCs) like for example cuprates provides an example of a stack of Josephson junctions, these are the so called intrinsic Josephson junctions. The layering scheme of such HTSCs is essentially the same, comprised of a stack of conduction layers held together by binding layers as shown in the two figuers below [3] for different materials. The layering along the c-axis of the unit cell is in the form of groups of copper oxide layers separated by layers of calcium or yttrium for example, these groups of CuO_2 are responsible for the superconducting

properties of the material. Between these CuO_2 groups are binding layers usually made of metal oxides.

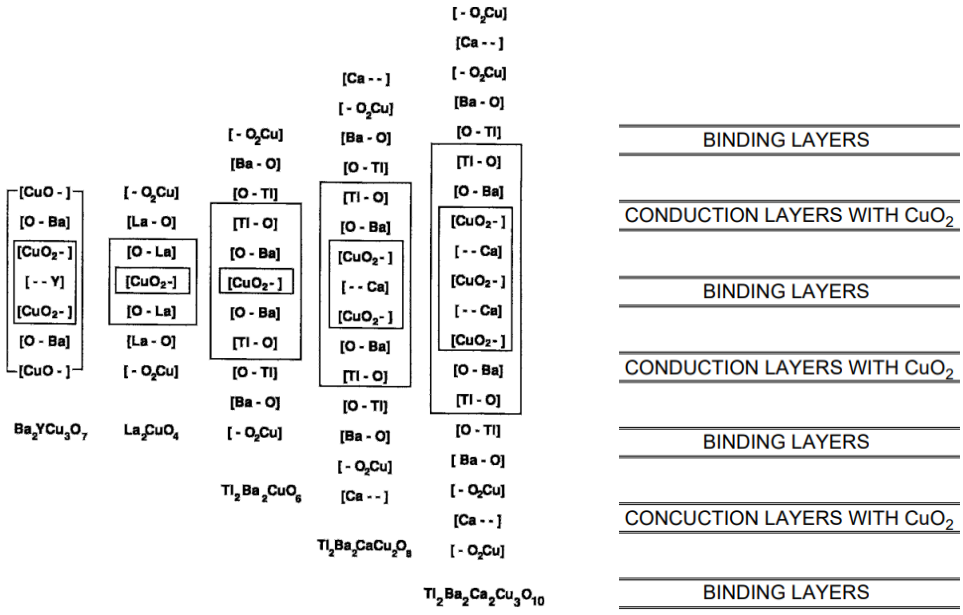

(a) (b)

Figure 2.1 [3] (a): Layering scheme for various cuprates where the large boxes constitute the unit cell and the small ones the conduction layers. (b): The general layering scheme.

2.2 CCJJ+DC model

Here we use the capacitively coupled Josephson junctions model with diffusion current (CCJJ+DC) [4] to study the CVC of our system of a stack of intrinsic Josephson junctions. Since the typical thickness of the superconducting layers is comparable to the Debye charge screening length this means that the electric charge isn't totally screened between layers leading to a capacitive coupling between them. Here we only use nearest neighbor coupling and the dimensionless Josephson equations are modified to be:

$$\frac{\partial \phi}{\partial \tau} = V_l - \alpha(V_{l+1} + V_{l-1} - 2V_l), \tag{2.1}$$

where the subscript l runs from 1 to $N+1$ specifying the number of the superconducting layer and α is the coupling parameter. The total current normalized to I_c takes the form

$$i = i_s^l + i_{qp}^l + i_D^l + i_{diff}^l + i_F, \tag{2.2}$$

where $i_s^l = \sin\phi_l$ is the Josephson supercurrent, $i_{qp}^l = \beta V_l$ is the quasiparticle current, $i_{qp}^l = \frac{dV_l}{d\tau}$ is the displacement current and an additional term stemming from Eq.(2.1) is the diffusion current $i_{diff}^l = -\alpha\beta(V_{l+1} + V_{l-1} - 2V_l)$ and thus

$$\frac{\partial V_l}{\partial \tau} = i - \sin\phi_l - \beta\frac{\partial \phi}{\partial \tau} + A\sin\omega\tau + i_F \tag{2.3}$$

where the additional term $A\sin\omega\tau$ accounts for the effect of the external radiation as before.
Here we impose periodic boundary conditions so that $V_{N+1} = V_1$ and use the same numerical method we used for a single SIS junction (see last paragraph in section 1.4) to solve Eqs.(2.1) and (2.3) for each superconducting layer.

2.3 Current voltage characteristics

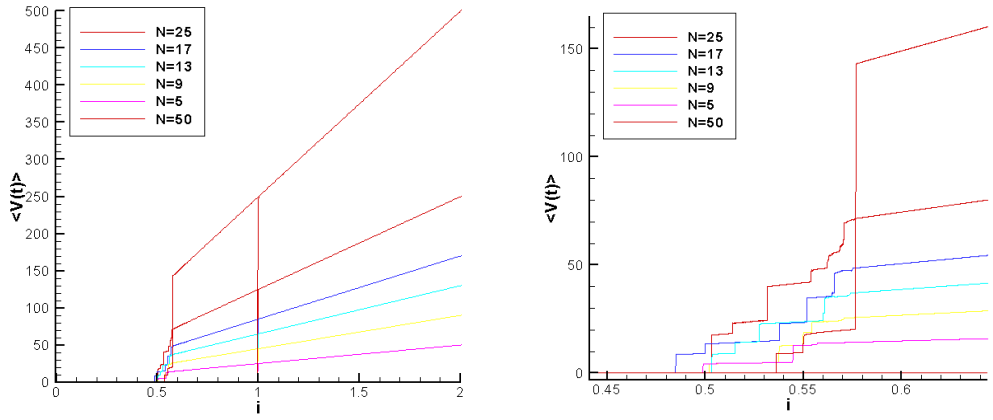

(a) (b)

Figure 2.2 (a): CVC for different values of N. (b): Zooming in on the area where the junctions switch one by one to the zero voltage state.

We first study the effect of changing the number of junctions N on the CVC for the underdamped case. We take the current step $\Delta i = 0.005$ and for the hysteresis region within $i_1 = 0.45$ and $i_2 = 0.65$ $\Delta i = 0.0001$, a step of time of $\Delta\tau = 0.05$ and a dissipation parameter of $\beta = 0.2$.
We notice that in the hysteresis region the transition to the zero voltage state happens gradually as each junction switches from the voltage state to the zero voltage state one by one till they all reside in the zero voltage state below a value of current we call the return current. We also notice that as the number of junctions increase the resistive branch is shifted higher and its slope increases.

2.4 Longitudinal plasma waves

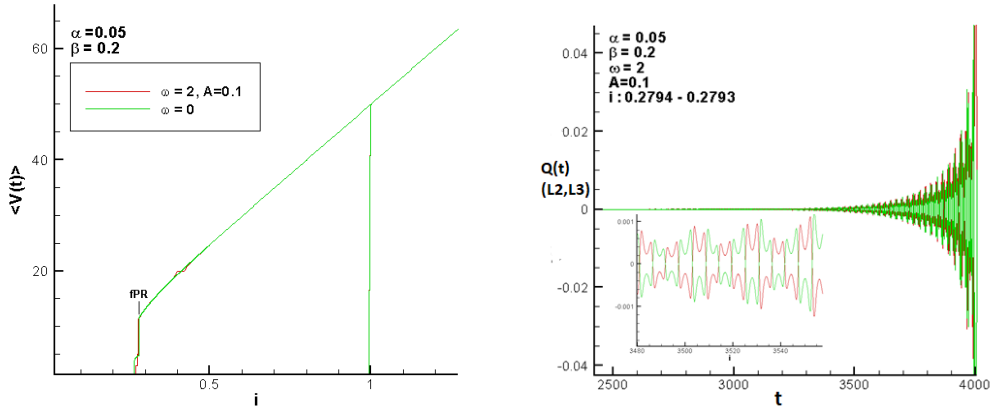

(a) (b)

Figure 2.3 (a): CVC for $\omega = 0$ and $\omega = 2, A = 0.1$. (b): Exponential charge growth at the fPR, inset shows charge on two neighboring layers being opposite to each other.

As we've mentioned earlier our system is characterized by a fPR where the electric charge on the superconducting layers grows exponentially and a longitudinal plasma wave whose frequency is half the Josephson oscillation frequency at that point is developed along the c-axis. Above are our CVC curves where the fPR is labeled and characterized by a breakpoint voltage $V_{bp} \simeq 11.51$ for $\omega = 0$ thus using Eq.(1.5) and for a number of junctions

of $N = 10$ the Josephson oscillation frequency normalized to the plasma frequency takes the value $\omega_J = V_{bp}/N \simeq 1.151$. It should be that V_{bp} for $\omega = 2$ and $A = 0.1$ is at a slightly lower value (visible when zoomed in). The model parameters we took are $\beta = 0.2$, $\alpha = 0.05$ and the numerical parameters $\Delta i = 0.005$ and within $i_1 = 0.2$ and $i_2 = 0.5$ $\Delta i = 0.0001$. The time domain for voltage averaging for $\omega = 0$ is from $\tau_1 = 50$ to $\tau_2 = 1000$ and for $\omega = 2$ from $\tau_1 \simeq 157$ to $\tau_2 \simeq 3141$.
Figure 2.3 (b) shows the exponential charge growth calculated according to the following normalized relation which directly follows from Gauss' law

$$Q_l = \alpha(V_{l+1} - V_l). \tag{2.4}$$

A longitudinal plasma wave (LPW) appears in the fPR along the c-axis of the stack where its wavelength is affected by the amplitude of the incident radiation as shown below. If we take the distance between two successive layers as d, Figure 2.4 shows a LPW of wavelength $2d$ for $A = 0$, $10d$ for $A = 0.15$ and $5d$ for $A = 0.23$.

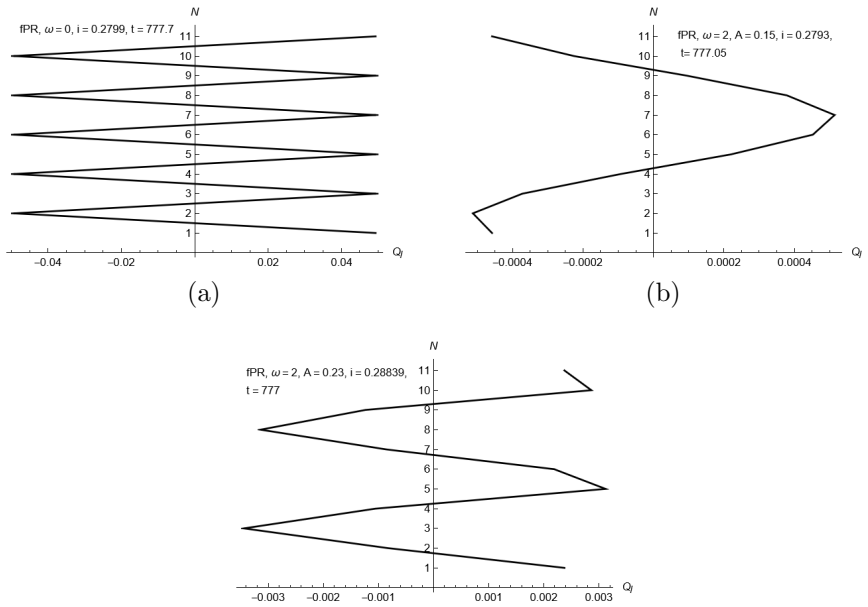

(a) (b) (c)

Figure 2.4 (a): LPW for $\omega = 0$, (b) $\omega = 2$ and $A = 0.15$ and (c) $\omega = 2$ and $A = 0.23$.

2.5 Double resonance

Here we observe the formation of shapiro steps within the fPR when the double resonance condition is reached, i.e. in addition to the fPR where $\omega_J = 2\omega_{LPW}$, the frequency of the incident radiation equals the Josephson oscillation frequency as well i.e.

$$\omega = \omega_J = 2\omega_{LPW}. \tag{2.5}$$

Since ω_J was found to be $\simeq 1.151$ for $\omega = 0$, Shapiro steps do not appear at lower frequencies, while for slightly higher frequencies they do appear as shown in the figures below.

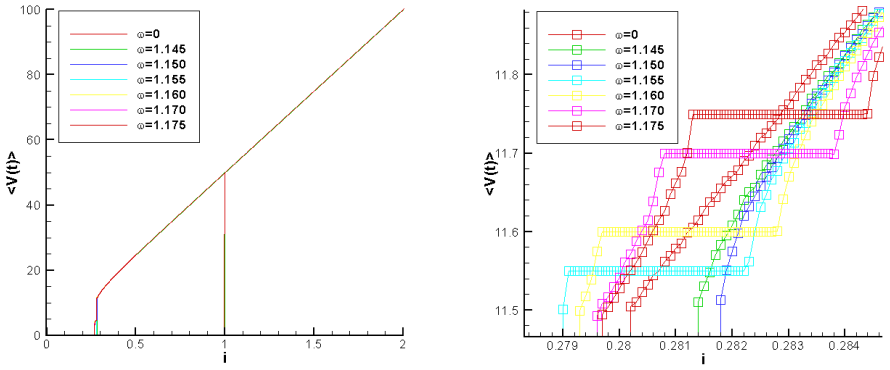

(a) (b)

Figure 2.5:(a) CVC for various values of ω and at $A = 0.005$, $\beta = 0.2$ and $\alpha = 0.05$., (b) A zoomed in fPR region showing the Shapiro steps.

2.6 Conclusion

In this study we were able to reproduce the data in [2] for a stack of SIS Josephson junctions, where we showed the development of a parametric resonance region where electric charge is produced on the superconducting layers and a LPW is developed. We also investigated the effect of the external radiation's amplitude on the wavelength of the LPW and observed the development of constant voltage steps (Shapiro steps) within the fPR region when the double resonance condition is satisfied, i.e. when the frequency of

incident radiation is equal to that of the Josephson oscillation frequency at the fPR.
We also studied the phase dynamics of a single SIS junction and studied the effect of external radiation on the CVC for the overdamped case where Shapiro steps appeared at normalized voltages which are integral multiples of the incident radiation's frequency normalized to the plasma frequency.

Acknowledgments

Firstly I would like to thank JINR for providing the INTEREST program for young researchers to earn a great research experience remotely within such short period of time to pave the way for their future work. I would also like to express my deepest gratitude to my supervisor, Dr. Majed Nashaat AbdelGhani for his patience, guidance and for unhesitatingly sharing all his knowledge to ease the way for us and make our learning experience as fruitful as possible. And lastly, special thanks to Prof. Yu. M. Shukrinov research group for providing me the code of calculations.

References

[1] Gross R, Marx A and Deppe F 2016 *Applied Superconductivity: Josephson Effect and Superconducting Electronics* De Gruyter Textbook (De Gruyter) ISBN 9783110417067

[2] Shukrinov Y M, Rahmonov I R and Gaafar M A 2012 *Physical Review B* **86**(18) 184502 ISSN 1098-0121

[3] Poole C, Farach H, Creswick R and Prozorov R 2007 *Superconductivity* 2nd ed (Academic Press)

[4] Shukrinov Y M and Rahmonov I R 2012 *Journal of Experimental and Theoretical Physics* **115**(2) 289–302 ISSN 1063-7761